Published OnlineFirst April 11, 2011; DOI: 10.1158/0008-5472.CAN-10-3775

Cancer Research

ErbB3 Ablation Impairs PI3K/Akt-Dependent Mammary Tumorigenesis

Rebecca S. Cook[1,3], Joan T. Garrett[2], Violeta Sánchez[2], Jamie C. Stanford[1], Christian Young[2], Anindita Chakrabarty[2], Cammie Rinehart[2], Yixian Zhang[4], Yaming Wu[4], Lee Greenberger[4], Ivan D. Horak[4], and Carlos L. Arteaga[1,2,3]

Abstract

The ErbB receptor family member ErbB3 has been implicated in breast cancer growth, but it has yet to be determined whether its disruption is therapeutically valuable. In a mouse model of mammary carcinoma driven by the polyomavirus middle T (*PyVmT*) oncogene, the ErbB2 tyrosine kinase inhibitor lapatinib reduced the activation of ErbB3 and Akt as well as tumor cell growth. In this phosphatidylinositol-3 kinase (PI3K)-dependent tumor model, ErbB2 is part of a complex containing PyVmT, p85 (PI3K), and ErbB3, that is disrupted by treatment with lapatinib. Thus, full engagement of PI3K/Akt by ErbB2 in this oncogene-induced mouse tumor model may involve its ability to dimerize with and phosphorylate ErbB3, which itself directly binds PI3K. In this article, we report that ErbB3 is critical for PI3K/Akt-driven tumor formation triggered by the *PyVmT* oncogene. Tissue-specific, Cre-mediated deletion of ErbB3 reduced Akt phosphorylation, primary tumor growth, and pulmonary metastasis. Furthermore, EZN-3920, a chemically stabilized antisense oligonucleotide that targets the ErbB3 mRNA *in vivo*, produced similar effects while causing no toxicity in the mouse model. Our findings offer further preclinical evidence that ErbB3 ablation may be therapeutically effective in tumors where ErbB3 engages PI3K/Akt signaling. *Cancer Res; 71(11); 3941–51. ©2011 AACR.*

Introduction

Gene mutations often dysregulate signaling pathways that control cell growth and survival, resulting in cancer formation. Several common oncogenic mutations converge to activate the phosphatidylinositol 3-kinase (PI3K) pathway, the most frequently altered network in human cancer (1). Activating mutations in *PIK3CA*, the gene encoding the p110α catalytic subunit of PI3K, have been reported in up to 40% of all breast cancers (2–6). Another mechanism of pathway disregulation is loss of the tumor suppressor gene phosphatase and tensin homolog deleted on chromosome 10 (*PTEN*), which negatively regulates PI3K output (7). A common mechanism of increased PI3K activity results from unrestrained receptor tyrosine kinase (RTK) activation. For example, amplification of the gene encoding ErbB2/HER2, found in approximately 25% of breast cancers, results in overexpression of the ErbB2–RTK, PI3K hyperactivity, and poor patient outcome (8, 9). PI3K induces phosphorylation and activation of Akt, a serine (Ser)/threonine (Thr) kinase that lies at the apex of a signaling cascade promoting tumor cell survival and proliferation (10).

Transgenic overexpression of the polyomavirus middle T (PyVmT) antigen in the mammary epithelium under the control of the *MMTV* promoter results in the formation of rapidly growing and highly metastatic mammary tumors (11, 12). MMTV–PyVmT mammary tumors exhibit many similarities to human breast cancer, including stochastic progression from benign hyperplasias to invasive, poorly differentiated carcinomas (13). PyVmT utilizes signaling pathways used by activated RTKs in human breast cancers (14), making it a useful model for understanding the signaling networks that contribute to multistage breast tumor progression. Although PyVmT lacks kinase activity, membrane-anchored PyVmT is phosphorylated on several tyrosine residues that recruit and bind PP2A, intracellular tyrosine kinases of the Src family (e.g., Src, Fyn, Yes), Shc, phospholipase C (PLC)-γ1, and the p85 regulatory subunit of PI3K (15). Activation of the PI3K/Akt pathway through p85 and the mitogen-activated protein kinase (MAPK) pathway through Shc results in increased cell survival and proliferation (16, 17). Similar to ErbB2-induced mammary tumors, PyVmT-mediated transformation requires PI3K/Akt, because a mutation abolishing the p85 interaction motif of PyVmT at Tyr315 impairs Akt activation and subsequent mammary tumor formation in transgenic mice (18). Therefore, the MMTV–PyVmT model lends itself to promote understanding of tumor cell dependence on PI3K.

Authors' Affiliations: Departments of [1]Cancer Biology and [2]Medicine, and [3]Breast Cancer Research Program, Vanderbilt-Ingram Cancer Center, Vanderbilt University School of Medicine, Nashville, Tennessee; and [4]Enzon Pharmaceuticals, Inc., Piscataway, New Jersey

Note: Supplementary data for this article are available at Cancer Research Online (http://cancerres.aacrjournals.org/).

Corresponding Author: Carlos L. Arteaga, Division of Oncology, Vanderbilt University Medical Center, 2220 Pierce Avenue, 777 PRB, Nashville, TN 37232. Phone: 615-936-3524; Fax: 615-936-1790; E-mail: carlos.arteaga@vanderbilt.edu

doi: 10.1158/0008-5472.CAN-10-3775

Published OnlineFirst April 11, 2011; DOI: 10.1158/0008-5472.CAN-10-3775

PyVmT-driven mammary tumors overexpress ErbB2 (18–20), but a contributing role of ErbB2 to middle T-induced tumor progression is unclear. Therefore, in this study, we examined whether expression and activity of ErbB2 and its heterodimeric partner ErbB3 are required for PyVmT-driven mammary transformation. Similar to PyVmT, ErbB3/HER3 lacks intrinsic kinase activity (8, 21). However, heterodimerization of ErbB2 and ErbB3 increases proliferation, survival, and transformation of breast cells more potently than any other ErbB receptor dimer (22, 23). Although ErbB2 does not directly engage PI3K, tyrosine-phosphorylated ErbB3 strongly engages PI3K through six p85 interaction motifs (24, 25), thus explaining the potent activation of PI3K/Akt by ErbB2/ErbB3 dimers.

In this study, we eliminated the expression and/or phosphorylation of ErbB3 in MMTV–PyVmT mammary glands and tumor cells using genetic and pharmacologic approaches. We found that conditional, temporally regulated loss of ErbB3 expression *in vivo* decreased PI3K/Akt signaling and the rate of tumor formation and metastasis in MMTV–PyVmT transgenic mice. Furthermore, use of a locked nucleic acid (LNA) ErbB3 antisense *in vivo* downregulated ErbB3 and p-Akt levels, prevented MMTV–PyVmT tumor formation in mice, inhibited established PyVmT tumor transplants, and inhibited growth of HER2-overexpressing human breast cancer cell lines *in vitro*. These results suggest that ErbB3 is an important component of PyVmT-mediated tumor formation and that stabilized high-affinity antisense ErbB3 oligonucleotides are a strategy worthy of clinical development against human tumors, such as HER2-overexpressing cancers, where ErbB3 engages PI3K/Akt.

Materials and Methods

Cells and culture conditions

HC11, BT-474, SKBR3, and MDA-MB-453 cells were purchased from the American Type Culture Collection (ATCC) and propagated according to ATCC specifications. Primary tumor cells from virgin female MMTV–Neu (26) and MMTV–PyVmT (11) mice were isolated as described previously (27, 28). Additional details, including ligands and inhibitors, are provided in Supplementary Materials and Methods.

Western analysis and immunoprecipitation

Western analysis and immunoprecipitation were done as described in Supplementary Materials and Methods.

Animal studies

All mice were housed in facilities that were approved by the Association for Assessment and Accreditation of Laboratory Animal Care under Institutional Animal Care and Use Committee guidelines in a pathogen-free environment. ErbB3$^{As/As}$ mice (referred to as ErbB3$^{fl/fl}$) have been described (29) and backcrossed more than 10 generations into the FVB genetic background. MMTV-Cre mice (30), TetOp-Cre (31), MMTV–rtTA (32), and MMTV–PyVmT (11) mice have been described previously. Mammary glands, tumors, and lungs from age-matched virgin female mice were used for analysis as described in Supplementary Materials and Methods.

Histologic analysis

Whole mammary glands were fixed on glass slides with neutral buffered formalin (Fisher Scientific) and stained with Mayer's hematoxylin (Fisher Scientific) as described previously (28). Additional details are provided in Supplementary Materials and Methods. Images were obtained using Olympus DP2 software on an Olympus light microscope. Minimal processing of images was done in Microsoft PowerPoint.

LNA oligonucleotides

These are described in Supplementary Materials and Methods.

Three-dimensional colony growth and TUNEL assays

Three-dimensional colony growth and terminal deoxynucleotidyl transferase–mediated dUTP nick end labeling (TUNEL) assays were done as described in Supplementary Materials and Methods.

Results

ErbB RTKs are required for MMTV–PyVmT tumor cell growth

Expression of ErbB2 and ErbB3 was increased in tumor cells derived from MMTV–PyVmT transgenic tumors compared with HC11 nontransformed mouse mammary epithelial cells and cells derived from MMTV–Neu mice that overexpress Neu, the rat homolog of ErbB2 (ref. 33; Fig. 1A). Treatment with 1 μmol/L lapatinib, a dual epidermal growth factor receptor (EGFR)/ErbB2 tyrosine kinase inhibitor (TKI; ref. 34), reduced basal and heregulin-induced phosphorylation of ErbB2, ErbB3, and Akt (Fig. 1B). The inhibition of ErbB3 phosphorylation was confirmed using site-specific Y1289 and Y1197 p-ErbB3 antibodies, which recognize 2 known p85/PI3K interaction motifs in the ErbB3 C-terminus (Fig. 1C). Lapatinib caused dose-dependent inhibition of MMTV–PyVmT colony growth in 3-dimensional (3D) Matrigel cultures, suggesting that PyVmT-driven tumor cells require signaling by ErbB receptors for growth (Fig. 1D). However, the EGFR TKI gefitinib (1 μmol/L) had no activity against MMTV–PyVmT tumor cell growth (data not shown), suggesting ErbB2, but not EGFR, plays a tumor-promoting role in these cells. Treatment with lapatinib of FVB mice bearing established MMTV–PyVmT tumor transplants significantly delayed tumor growth compared with control mice, thus confirming the role of ErbB2 *in vivo* (Fig. 1E). Ki67 immunoreactivity, a marker of cell proliferation, was markedly reduced in lapatinib-treated samples (Supplementary Fig. S1).

Because ErbB2 does not bind p85 directly, the inhibition of p-Akt in lapatinib-treated cells (Fig. 1B) suggested the presence of an ErbB2-dependent p-ErbB3/p85 complex which, in turn, activated PI3K/Akt. Indeed, ErbB3 and p85 immunoprecipitate from tumor cell lysates recovered p85 and ErbB3, respectively, supporting the association of both molecules under basal conditions (Fig. 1F, lanes 1 and 3). Treatment with lapatinib markedly reduced the association of p85 with ErbB3 (Fig. 1F, lanes 2 and 4). Middle T and

Published OnlineFirst April 11, 2011; DOI: 10.1158/0008-5472.CAN-10-3775

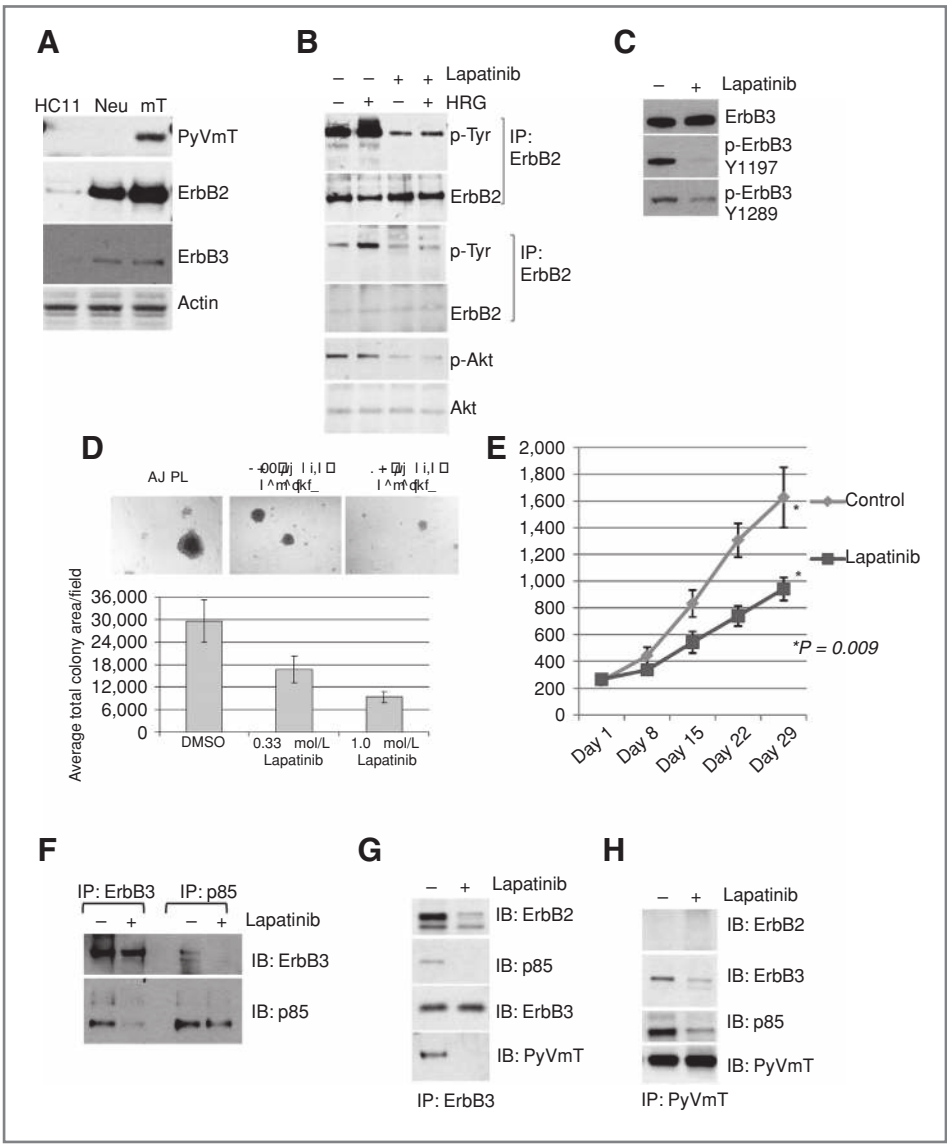

Figure 1. Inhibition of ErbB2 impairs growth of MMTV–PyVmT tumors. A, whole-cell extracts prepared from HC11 mouse mammary cells or MMTV–Neu (Neu) and MMTV–PyVmT (mT) primary tumor cells were analyzed by immunoblotting for the proteins indicated at the right of each panel. B and C, whole-cell extracts from MMTV–PyVmT primary tumor cells cultured in serum-free media for 6 hours ± lapatinib (1 μmol/L) and an additional 5 minutes ± heregulin (HRG; 2 ng/mL; in B) were used for Western blot analysis or for immunoprecipitation (IP) followed by Western blot analysis to detect the proteins indicated at the right of each panel. D, MMTV–PyVmT cells were embedded in growth factor–reduced Matrigel with increasing concentrations of lapatinib. Medium and lapatinib were replenished every 2 days. Digital images were analyzed with Olympus DP2 software to measure colony area in pixels. At least 50 colonies per well × 3 wells per condition were measured and used to calculate the average colony size per well. Values represent the average total colony area per well ± SD. E, MMTV–PyVmT primary tumors cells (1×10^6) were injected into the inguinal mammary fat pad of 5-week-old wild-type FVB female mice. Tumor-bearing mice (tumor volume ≥200 mm^3) were treated ± lapatinib (100 mg/kg/d × 28 days). Tumor volume was measured weekly as indicated in Materials and Methods section. Each data point represents the mean tumor volume in mm^3 ± SD ($n = 10$; $P = 0.0021$, Mann–Whitney *U* test). F–H, whole-cell extracts from MMTV–PyVmT primary tumor cells cultured in serum-free media with lapatinib (1 μmol/L) for 24 hours were used for IP with antibodies against the following: ErbB3 and p85 (F), ErbB3 (G), and PyVmT (H). Immune complexes were separated by SDS–PAGE and next subjected to immunoblot (IB) analysis using the indicated antibodies as described in Materials and Methods section.

ErbB2 were constitutively associated with ErbB3 (Fig. 1G). This basal association between ErbB3 and PyVmT was reduced on inhibition of the ErbB2 kinase with lapatinib. In converse experiments using immunoblot analysis of mT antibody pull-downs, ErbB3 was recovered from PyVmT immune complexes in untreated cells, but not from lapatinib-treated cells (Fig. 1H), and the total level of p85 in association with PyVmT was reduced, suggesting ErbB2 kinase activity is required for maintenance of this signaling complex.

Published OnlineFirst April 11, 2011; DOI: 10.1158/0008-5472.CAN-10-3775

Mammary-specific deletion of ErbB3 delays PyVmT-induced mammary tumors

To determine the role of ErbB3 on cancer formation in MMTV–PyVmT mice, we eliminated ErbB3 in the mammary epithelium using MMTV-Cre (MCre) transgenic mice (30) and mice harboring floxed *ErbB3* alleles (29). In these mice (referred to hereafter as PyVmT × ErbB3$^{fl/fl}$.MCre mice), Cre induces genomic recombination at the floxed *ErbB3* locus. ErbB3$^{fl/fl}$ mice were backcrossed with FVB mice for more than 10 generations, placing the mice on identical genetic backgrounds as MMTV–Cre and MMTV–PyVmT mice. Mammary glands from PyVmT × ErbB3$^{fl/fl}$.MCre mice harvested at 8 weeks of age showed markedly decreased formation of multifocal mammary neoplasms (Fig. 2A). At later time points, all targeted and control mice formed mammary tumors. However, loss of ErbB3 delayed average tumor latency [T_{50} = 57.5 vs. 42.5 days in ErbB3-deficient vs. heterozygous and wild-type controls; $P < 0.0001$, log-rank test; Fig. 2B]. Histologic lung sections taken at 100-μm intervals revealed micrometastases in 100% of PyVmT × ErbB3$^{+/+}$.MCre, 69% of PyVmT × ErbB3$^{fl/+}$.MCre, and 62% of PyVmT × ErbB3$^{fl/fl}$.MCre mice. However, the average number of metastases per lung was statistically diminished in PyVmT × ErbB3$^{fl/fl}$.MCre mice as compared with ErbB3 heterozygotes (Fig. 2C). At the time of euthanasia (11 weeks of age), the combined wet weight of all 10 tumor-bearing mammary glands in each mouse was measured (Fig. 2D), revealing a significant decrease in the average total tumor weight in PyVmT × ErbB3$^{fl/fl}$.MCre mice (3.73 ± 0.99 g) as compared with PyVmT × ErbB3$^{fl/+}$.MCre mice (5.93 ± 1.88 g; $n = 6$, $P = 0.015$, Student unpaired t test).

Tumor-bearing mammary glands harvested from mice at 11 weeks of age revealed cystic hyperplasias and low-grade ductal carcinomas *in situ* (DCIS) in PyVmT × ErbB3$^{fl/fl}$.MCre samples, whereas heterozygous samples harbored malignant, poorly differentiated solid sheets of tumor cells (Fig. 2E). TUNEL analysis revealed an increase in apoptotic nuclei in ErbB3-deficient hyperplasias. Immunoblot analysis of whole PyVmT × ErbB3$^{fl/fl}$.MCre tumor lysates confirmed a marked reduction in ErbB3 content compared with lysates from tumors lacking Cre or floxed *ErbB3* alleles (Fig. 2F). S473 p-Akt was reduced in lysates from ErbB3-deficient tumors (Fig. 2F). Immunoprecipitation of p85 coprecipitated PyVmT in tumors from PyVmT × ErbB3$^{fl/+}$.MCre mice, but not from ErbB3-deficient tumors (Fig. 2G), suggesting that ErbB3 contributes to the association of p85 with middle T and the activation of PI3K in tumors *in vivo*.

ErbB3 antisense EZN-3920 prevents mammary tumor formation

EZN-3920 is an LNA antisense with target specificity to human and mouse ErbB3 (35). LNA-based oligonucleotides have 14- to 16-mer sequences and exhibit high mRNA affinity, stability in plasma and against nucleases, and tissue residence time of several days (36–39). Treatment of MMTV–PyVmT cells with EZN-3920 but not its mismatch control EZN-4455 for 3 days reduced ErbB3 protein levels but did not affect ErbB2, ErbB4, or EGFR expression (Fig. 3A, top). Of note, EZN-4455 is not a fully scrambled molecule but a 3-bp mismatch (5′-tag ctt gtc cca tct c-3′ vs. 5′-tag cct gtc act tct c-3′ in EZN-3920). Consistent with ErbB3 knockdown, the basal association of p85 and ErbB3 was eliminated in cells treated with EZN-3920 (Fig. 3A, bottom). MMTV–PyVmT female mice were treated twice weekly with EZN-3920 for 5 weeks (i.e., 10 doses), beginning at 3 weeks of age. Tissues were collected 24 hours after the final dose. Histologic sections from mice treated with the mismatch EZN-4455 revealed total replacement of the mammary glands with tumor cells (Fig. 3B). In contrast, mammary tumor formation was inhibited in mice treated with EZN-3920 such that architecture of the gland was preserved (Fig. 3C), including single layered epithelial ductal structures (Fig. 3D). Mammary hyperplasias were still evident in the proximal one third of glands of mice treated with EZN-3920 (Supplementary Fig. S2). Immunohistochemical levels of S473 p-Akt were reduced more than 60% in tumors from mice treated with EZN-3920 than in those treated with EZN-4455 (Fig. 3E and F). These data are consistent with the notion that ErbB3 contributes to PyVmT-induced PI3K/Akt and tumor progression.

Genetic and pharmacologic ablation of ErbB3 inhibits growth of established MMTV–PyVmT tumors

To examine the consequences of acute loss of ErbB3 on progression of established PyVmT-driven tumors, we used a tetracycline/doxycycline-inducible model of mammary-specific Cre recombinase expression to impair ErbB3 expression in MMTV–PyVmT mice. The double transgenic model referred to as *MTB-TCre* combines MMTV–rtTA (32) and TetOp-Cre transgenic mice (30). Treatment of PyVmT × ErbB3$^{fl/fl}$.MTB-TCre primary tumor cells with tetracycline reduced ErbB3 and S473 p-Akt levels (Fig. 4A). PyVmT × ErbB3$^{fl/fl}$.MTB-TCre primary tumor cells were orthotopically transplanted in wild-type FVB mice. Mice remained naïve to doxycycline until tumor volume reached ~50 mm^3, at which time they received doxycycline for 1 week. Mice were then either withdrawn from doxycycline or maintained on doxycycline for the following 7 weeks. After 8 weeks of continuous doxycycline treatment, the average volume of PyVmT × ErbB3$^{fl/fl}$.MTB-TCre tumors was 808 ± 63 mm^3 compared with 1,650 ± 487 mm^3 in doxycycline-naïve mice (Fig. 4B). A modest but statistically significant reduction in final tumor volume was seen in mice treated for the full duration of 8 weeks with doxycycline as compared with those treated for only 1 week followed by 7 weeks without doxycycline. These data are not only consistent with the irreversible nature of recombination at the targeted ErbB3 allele but also suggest the presence of cells escaping Cre-mediated recombination after only a week of doxycycline treatment. Western analysis of whole tumor lysates confirmed doxycycline-inducible, Cre-mediated loss of ErbB3 *in vivo*, correlating with an overall reduction in the content of S473 p-Akt (Fig. 4C). Immunohistochemistry (IHC) also showed a marked reduction in ErbB3 protein levels in doxycycline-treated compared with doxycycline-naïve tumors (Fig. 4D).

In addition to the conditional deletion of ErbB3 in the genetic model, we used a pharmacologic approach to ablate ErbB3 in established tumors. Syngeneic nontransgenic FVB

Published OnlineFirst April 11, 2011; DOI: 10.1158/0008-5472.CAN-10-3775

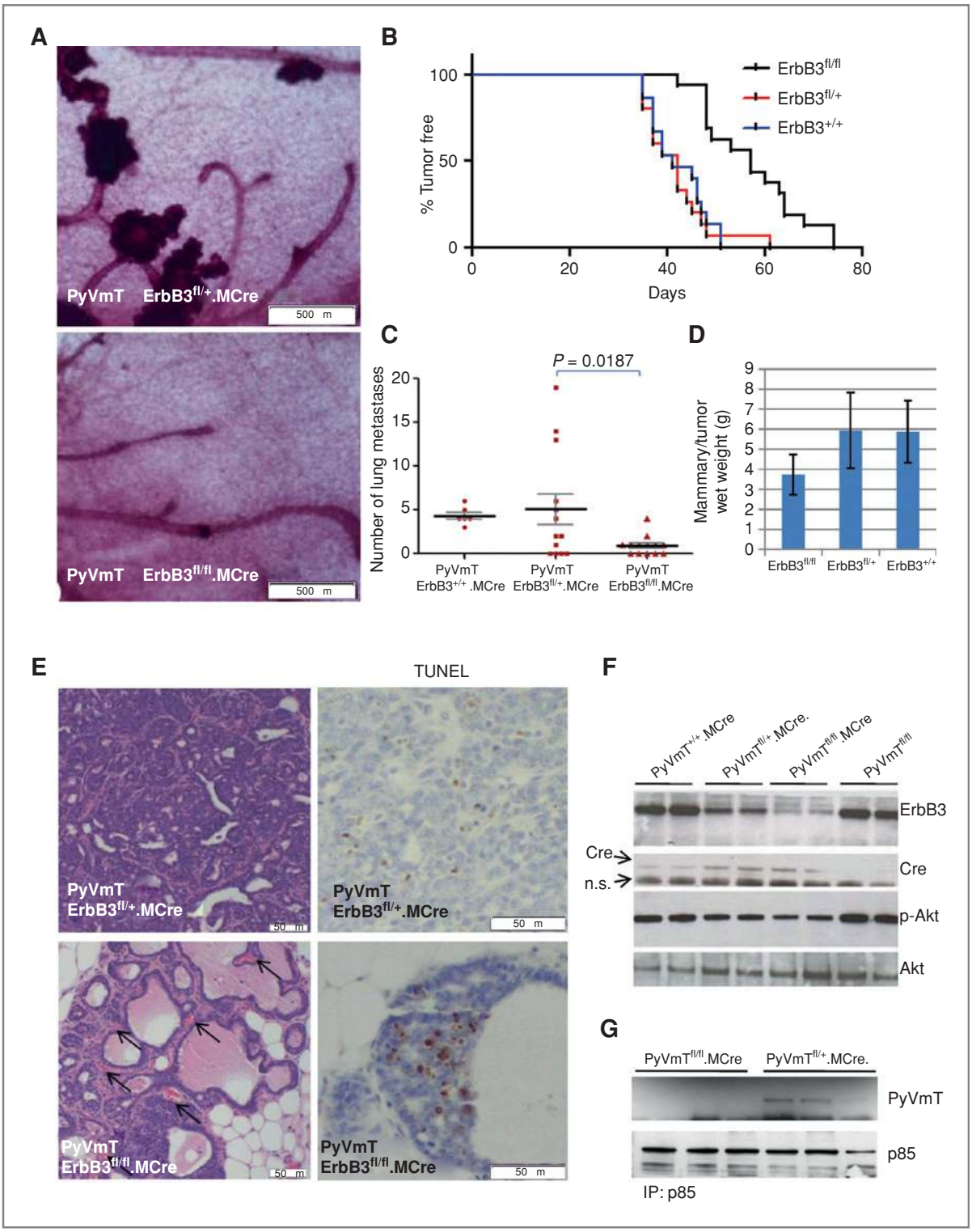

Figure 2. Absence of ErbB3 impairs the formation of MMTV–PyVmT multifocal tumors. A, whole-mount hematoxylin-stained inguinal mammary glands of 8-week-old virgin female mice. B, tumor-free curve was generated by documenting the time at which tumors were originally palpated. The average tumor latency (T_{50}) was calculated using the Kaplan–Meier test ($n = 20$ for each genotype; $P < 0.0001$, log-rank test). C, lung metastases were identified in histologic sections and enumerated. The midlines indicate the average number of lung metastases for each genotype ± SD. D, 10 mammary glands per mouse were harvested and weighed together. The values show the average total mammary/tumor wet weight ± SE ($n = 6$; $P = 0.015$). E, Hematoxylin and eosin (H&E)–stained tumor sections (left) and TUNEL-stained tumor sections (right) from 11-week-old virgin female mice. F, whole-tumor lysates were prepared as described in Materials and Methods section and used for Western blot analysis with the antibodies indicated at the right of the panels. Genotype of each tumor (with respect to the targeted *Erbb3* and *MMTV-Cre* alleles) is indicated at the top. n.s., nonspecific. G, whole-tumor extracts harvested from 3 mice per genotype were precipitated with a p85 antibody. Immune complexes were separated by SDS–PAGE followed by Western analysis for p85 and PyVmT as indicated in Materials and Methods section.

Published OnlineFirst April 11, 2011; DOI: 10.1158/0008-5472.CAN-10-3775

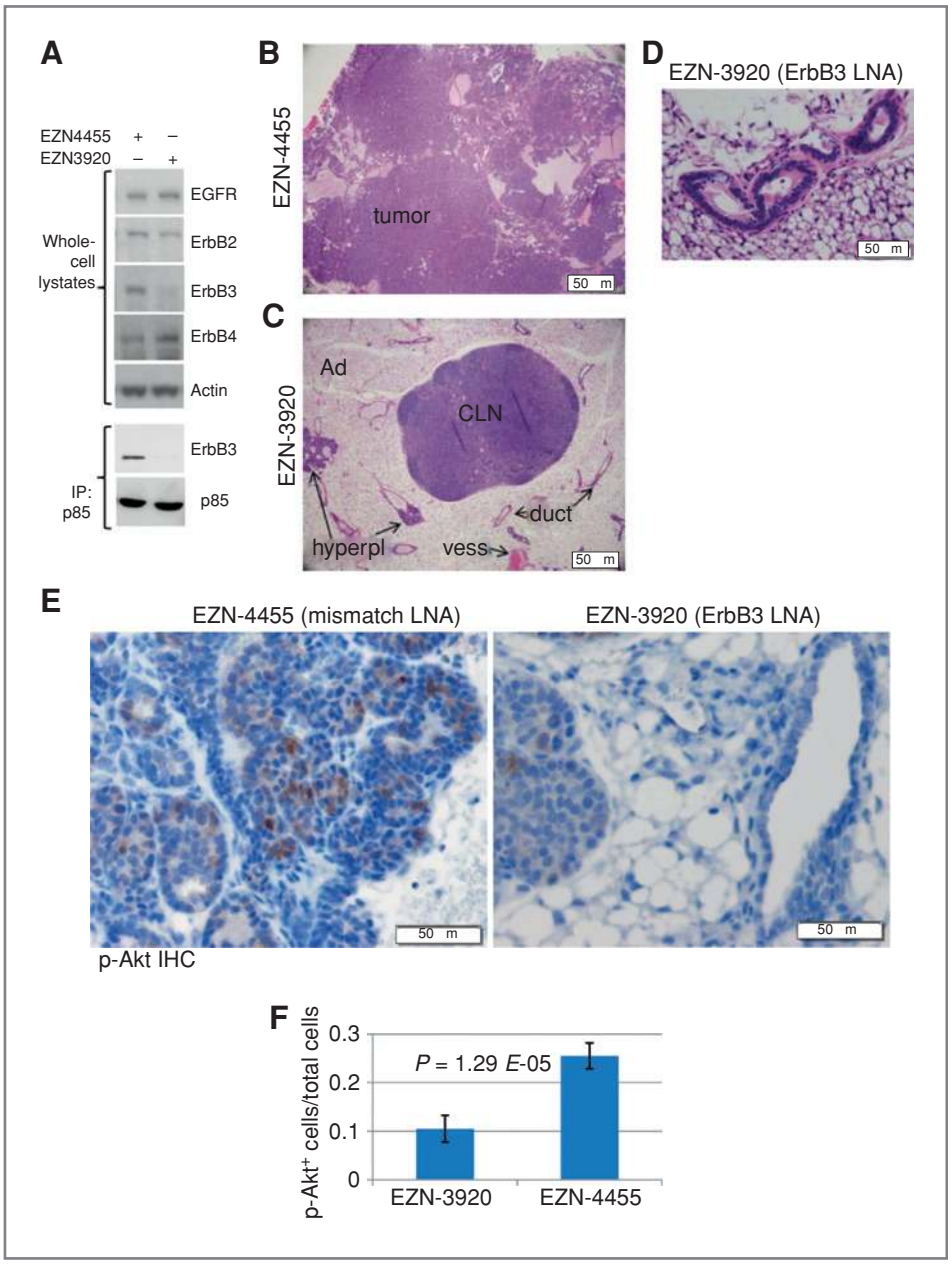

Figure 3. EZN-3920 inhibits tumor formation and p-Akt in mammary glands of MMTV–PyVmT mice. A, primary MMTV–PyVmT tumor cells were treated in culture with 2.5 μmol/L EZN-3920 or EZN-4455 for 72 hours. Whole-cell extracts were used directly for Western blot analysis to detect expression of ErbB3, ErbB2, and EGFR or used for p85 immunoprecipitation (IP) followed by Western blot analysis for ErbB3 and p85. B–F, treatment with EZN-4455 or EZN-3920 (25 mg/kg, twice weekly) began when mice were 3 weeks old and continued for 5 weeks (total of 10 doses). Tissues were harvested 24 hours after the final dose was administered. B and C, low-power magnification of inguinal mammary glands of mice treated with EZN-4455 (B) or EZN-3920 (C) illustrates profound inhibition of tumor progression in mice treated with EZN-3920. CLN, central lymph node; Ad, adipose tissue; duct, normal ductal epithelium; vess, blood vessel; hyperpl, hyperplastic nodule. D, high-power magnification of mammary epithelium from mouse treated with EZN-3920. Note single layer of epithelium surrounding a lumen. E, IHC detection of S473 p-Akt. F, quantitation of the rate of p-Akt positivity in mammary epithelium of mice treated with EZN-4455 and EZN-3920. Values represent the average number ± SD of p-Akt$^+$ epithelial cells per total number of epithelial cells in five 400× fields per sample × 5 samples per condition ($P = 0.00001$; Student unpaired t test).

mice bearing established MMTV–PyVmT tumors (~200 mm^3) were treated twice weekly with EZN-3920 or EZN-4455 for 4 weeks (i.e., 8 doses). Treatment with the ErbB3 antisense EZN-3920 decreased tumor volume by more than 60% compared with EZN-4455–treated tumors (Fig. 5A; $P = 0.002$, Student t test). IHC confirmed a marked reduction of detectable ErbB3 expression in tumors treated with EZN-3920 (Fig. 5B). Histologic examination of tumors harvested 24 hours after the last of 8 doses revealed extensive acellular debris and extracellular matrix with a scarcity of cancer cells in the ErbB3-deficient tumors (Fig. 5C). In contrast, control tumors exhibited solid sheets of poorly differentiated tumor cells with central regions of necrosis. S473 p-Akt was abundant in EZN-4455–treated tumors but substantially decreased in the actively growing areas of EZN-3920–treated tumors (Fig. 5D). At this late time point (4 weeks of therapy), we did not detect differences in the rate of tumor cellular proliferation as measured by Ki67 between both treatment groups (Fig. 5E).

ErbB3 ablation with EZN-3920 increases response to lapatinib in ErbB2 gene–amplified human breast cancer cells

Finally, we examined the impact of ErbB3 ablation in human breast cancer cell lines harboring *ErbB2* gene amplification. Transfection of BT-474 and SKBR3 cells with EZN-3920

Published OnlineFirst April 11, 2011; DOI: 10.1158/0008-5472.CAN-10-3775

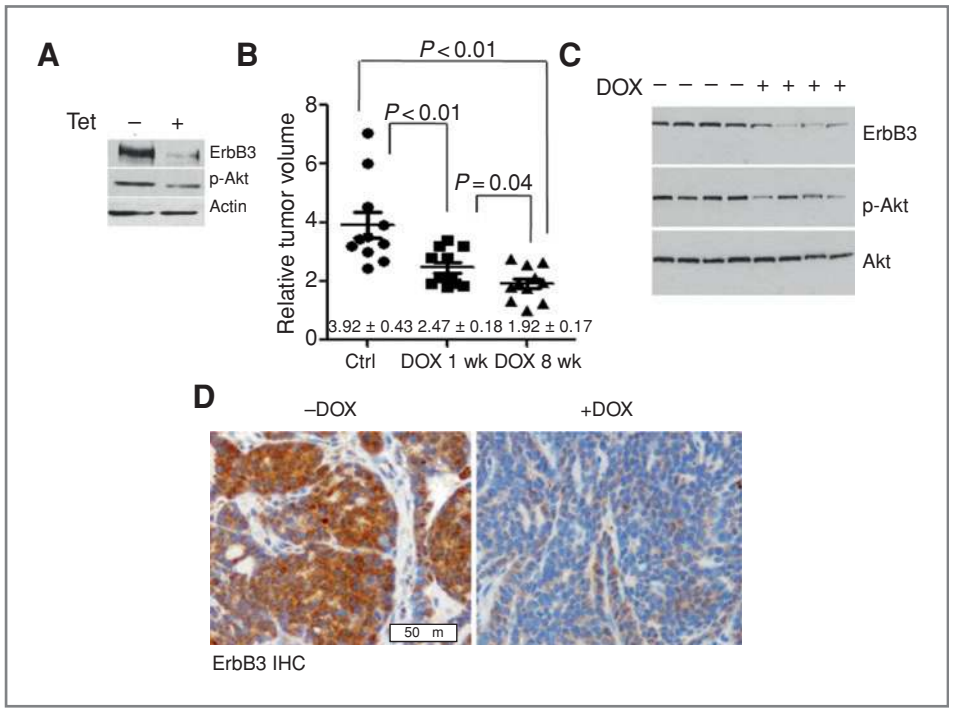

Figure 4. Genetic ablation of ErbB3 inhibits growth of PyVmT tumors. A, PyVmT × ErbB3$^{fl/fl}$.MTB–TCre primary tumor cells were treated with tetracycline (Tet) for 9 days; whole-cell lysates were prepared and analyzed by Western blot to detect ErbB3, p-Akt, and β-actin (control). B, PyVmT × ErbB3$^{fl/fl}$.MTB–TCre primary tumor cells were injected into the inguinal mammary fat pad of wild-type female FVB mice. When tumors reached a size of ~50 mm^3, mice were randomized into treatment groups receiving doxycycline (DOX) for an 8-week period or receiving doxycycline for 1 week followed by doxycycline removal for the remaining 7 weeks of the study. The third group did not receive doxycycline. Tumor volume was calculated at the end of the 8-week treatment period. Values shown represent the average tumor volume relative to the volume of the tumor with the smallest volume (144 mm^3). Ctrl, control. C, Western blot analysis of whole tumor lysates harvested from mice at the end of the 8-week period of treatment with doxycycline. Antibodies used for Western blot analysis are shown at right of each panel. D, IHC detection of ErbB3 in tumors from doxycycline-treated mice. Tumors shown are from mice maintained on doxycycline for 8 weeks or not.

(5 μmol/L) decreased ErbB3 protein expression as well as basal association of p-ErbB3 with p85 (Fig. 6A). Next, BT-474, SKBR3, and MDA-MB-453 cells were treated with EZN-3920 before being embedded in 3D Matrigel cultures. After 14 days of 3D culture, cells treated with EZN-4455 formed abundant colonies in Matrigel (Fig. 6B). However, cells treated with EZN-3920 to inhibit ErbB3 expression produced colonies that were fewer and smaller.

Because ErbB2 is the main stimulus of ErbB3 tyrosine phosphorylation in ErbB2-overexpressing cells, we studied the combined effect of inhibiting ErbB2 and ErbB3. Although EZN-3920 could not induce apoptotic cell death when used alone, the combination of EZN-3920 with lapatinib induced more apoptosis than with lapatinib alone or lapatinib plus the anti-HER2 antibody trastuzumab (Fig. 6C). To further confirm target inhibition by EZN-3920, we examined levels of total ErbB3 and p-ErbB3. BT-474, SKBR3, and MDA-MB-453 cells treated with lapatinib responded initially with a decrease in Y-1997 p-ErbB3 (at 1 and 4 hours), consistent with inhibition of ErbB2 kinase activity (Fig. 6D). However, within 24 hours, p-ErbB3 and total ErbB3 recovered partially. However, in cells treated with lapatinib and EZN-3920, the recovery of ErbB3 and p-ErbB3 was markedly reduced (Fig. 6D), potentially explaining the additive effect on cell growth.

Discussion

The ErbB3 (HER3) receptor lacks tyrosine kinase activity but can potently activate the PI3K/Akt signaling pathway via its 6 docking sites for the p85 subunit of PI3K (21, 24, 25). Several oncogenic RTKs, such as ErbB2, MET, FGFR2, and EGFR, phosphorylate ErbB3 to engage PI3K (reviewed in refs. 8, 40), and this activation has been shown to be critical for oncogene-induced transformation and/or drug resistance. For example, loss of ErbB3 by different genetic manipulations impairs viability of ErbB2-dependent human breast cancer cells, suggesting that the ErbB2 oncogene depends on ErbB3 to maintain growth and survival (22, 41). Lung cancer cells with acquired resistance to the EGFR TKI gefitinib overexpress MET, which results in ErbB3 phosphorylation and PI3K/Akt activation. In these cells, knockdown of ErbB3 with short hairpin RNAs inhibits PI3K/Akt and restores sensitivity to the EGFR inhibitor (42). These data suggest that inhibition of ErbB3 in combination with oncogene-targeted therapies may be an effective approach to prevent acquired resistance or improve tumor response.

As a therapeutic target, ErbB3 presents with the challenge of having an inactive tyrosine kinase, thus precluding the utility of ATP-mimetic TKIs. Circumventing this challenge are

Published OnlineFirst April 11, 2011; DOI: 10.1158/0008-5472.CAN-10-3775

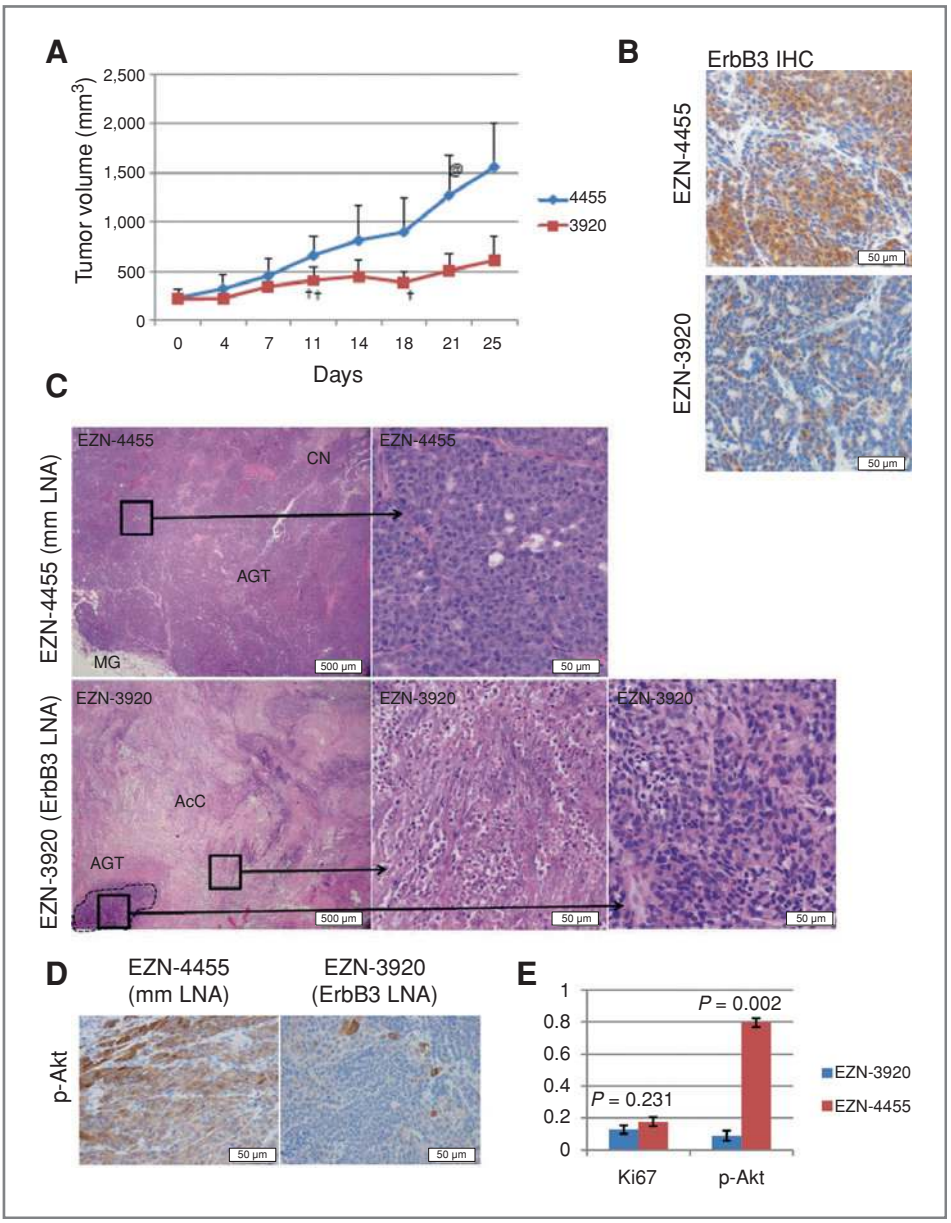

Figure 5. Systemic delivery of ErbB3 antisense inhibits growth of established MMTV–PyVmT mammary tumors. A, MMTV–PyVmT primary tumor cells were injected into the inguinal mammary fat pad of 5-week-old wild-type FVB mice. When tumors reached a volume of 200 mm^3 or more, mice were randomized to receive 25 mg/kg EZN-3920 or EZN-4455 twice weekly via tail-vein injection. Tumor volumes were monitored twice weekly and were calculated as indicated in Materials and Methods section. Each data point represents the mean tumor volume ± SD ($n = 7$; $P = 0.006$, Student t test). †, identification of dead mouse in cage; @, mouse removed from study because of excessive tumor volume. B–E, tumors were harvested 24 hours after the final of 8 doses and examined histologically. B, IHC detection of ErbB3 as described in Materials and Methods section. C, H&E-stained sections of tumors. Left, lower magnification. Right, boxed areas in higher-power magnification. Two boxed areas are indicated in the EZN-3920 samples to show the acellular compartment (AcC) and the area of actively growing tumor (AGT). D, IHC detection of S473 p-Akt. E, the index of cells staining positive for p-Akt and Ki67 was calculated as the number of positive cells divided by the total number of cells. Five randomly chosen fields from each of 5 samples were counted. Values represent the average ± SD.

antibody-mediated strategies aimed at blocking ligand binding to ErbB3 (e.g., MM-121; ref. 43) or blocking the dimerization of ErbB3 with ErbB2 in ErbB2-overexpressing cells (e.g., pertuzumab; ref. 44). Although each of these strategies have met with some success in preclinical (43, 45) and clinical studies (46, 47), they are theoretically limited by their inability to block phosphorylation of ErbB3 by amplified heterologous tyrosine kinases (40). For example, in non–small-cell lung cancers (NSCLC), ErbB3 can be phosphorylated by the amplified MET receptor, leading to resistance to EGFR TKIs (42). Furthermore, ErbB3 was a substrate for FGFR2 in *FGFR2*-amplified gastric cancer cells (48). In these scenarios, binding to the ectodomain of ErbB3 may do little to inhibit the interaction of ErbB3 with MET or FGFR2. Our results show that LNA oligonucleotides targeting ErbB3 mRNA downregulate ErbB3 in tumors and inhibit their growth *in vivo*, thus representing a targeting strategy that warrants further investigation, particularly in ErbB2-overexpressing cancers. In these tumors, modulation *in situ* of surrogate pharmacodynamic biomarkers of PI3K activity (e.g., p-Akt, p-PRAS40) simultaneously with ErbB3 levels can be used to assess therapy-induced targeted inhibition of ErbB3. The studies shown herein validate the potential of targeted ErbB3 ablation *in vivo* using LNA oligonucleotides. Although previous studies showed accumulation of LNA oligonucleotides in liver and kidney (L. Greenberger, personal communication), we have shown the utility of LNA-based antisense oligonucleotides to downregulate target gene expression in normally developing mammary tissue and in tumors that develop within the native mammary gland environment.

Published OnlineFirst April 11, 2011; DOI: 10.1158/0008-5472.CAN-10-3775

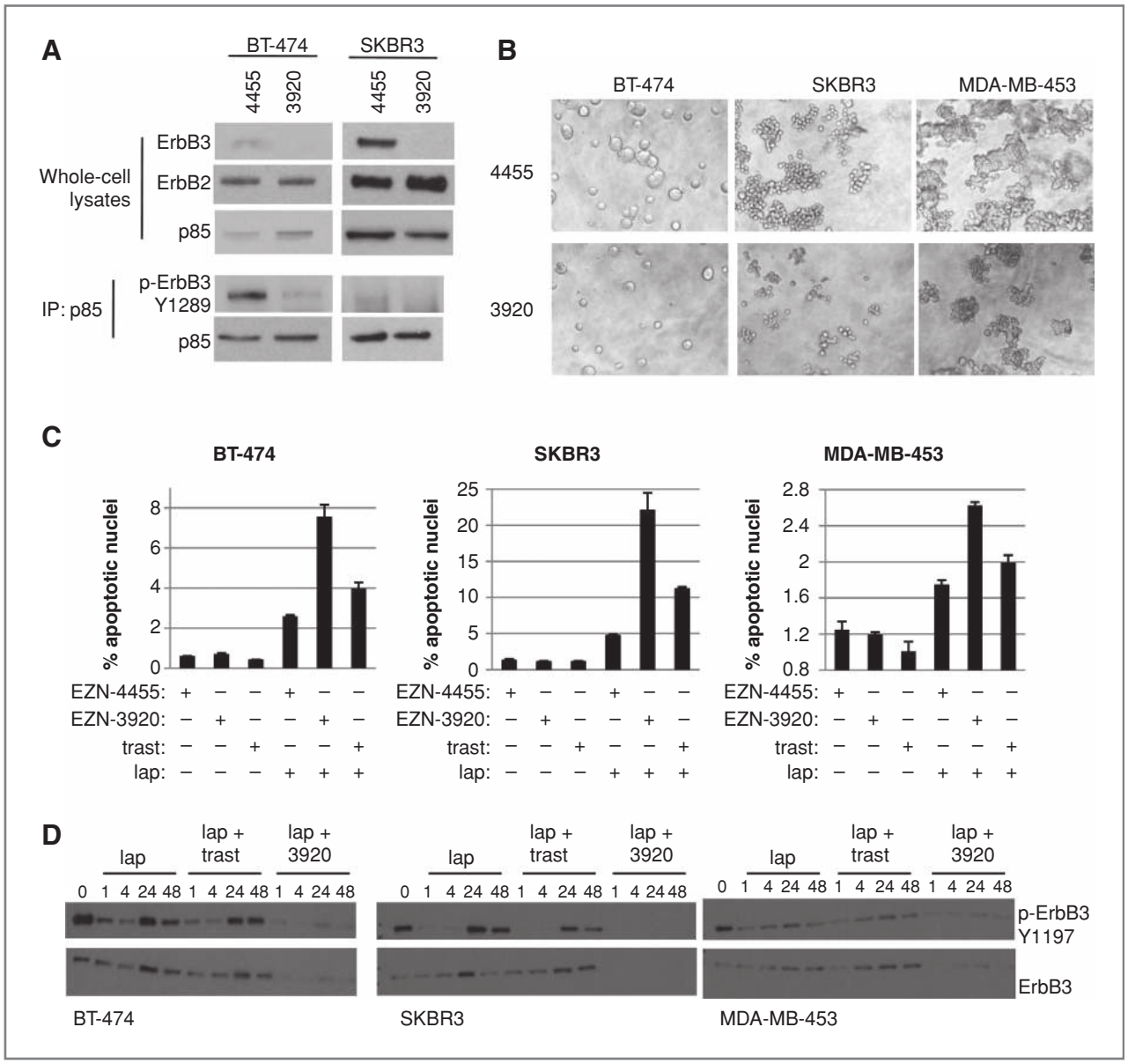

Figure 6. ErbB3 ablation with EZN-3920 cooperates with lapatinib (lap) to induce tumor cell death. A, cells were treated with EZN-4455 or EZN-3920 for 6 days before harvesting whole-cell extracts, which were used directly for Western blot analysis or for immunoprecipitation (IP) of p85 followed by Western blot analysis. B, cells were transfected with EZN-3920 or EZN-4455 (5 μmol/L) and then embedded in growth factor–reduced Matrigel. Cells were imaged at day 14. C, cells cultured in monolayer were transfected with EZN-3920 or EZN-4455 (5 μmol/L) for 72 hours. Cells were treated for the final 16 hours with trastuzumab (trast; 20 μg/mL), lapatinib (1 μmol/L) or DMSO. Cells were fixed and stained for evidence of apoptosis, using the APO-bromodeoxyuridine assay, and measured using flow cytometry. Values shown represent the average percentage of the cell population that was TUNEL-positive, ± SEM ($n = 3$; lapatinib vs. EZN-3920 plus lapatinib; $P < 0.01$ for BT-474, SKBR3, and MDA-MB-453 cells). lap, lapatinib; trast, trastuzumab. D, cells were transfected with EZN-3920 or EZN-4455 (5 μmol/L) for 72 hours. Cells were treated for the final 1, 4, 24, or 48 hours of culture with lapatinib (1 μmol/L) in the presence of absence of trastuzumab (20 μg/mL) or with DMSO. Whole-cell extracts were analyzed by Western blot analysis with Y1197 p-ErbB3 and total ErbB3 antibodies.

The carboxy-terminal tail of ErbB3 has 6 YXXM motifs that when phosphorylated engage the N-SH_2 domain of p85, thus activating the p110 catalytic subunit of PI3K (8). PyVmT interacts with p85 through a single YXXM (13). Mutation of this single motif impairs the ability of PyVmT to activate PI3K signaling, thus decreasing the oncogenicity of PyVmT (18). Given that both ErbB3 and PyVmT use p85, it is possible that these 2 proteins would compete for limiting levels of p85. Data presented herein suggest that p-ErbB3 does not compete with PyVmT for p85, because ErbB3, p85, and PyVmT were found in a common complex (Fig. 2). This interaction appeared to be dependent on

Published OnlineFirst April 11, 2011; DOI: 10.1158/0008-5472.CAN-10-3775

ErbB2, as the TKI lapatinib inhibited assembly of PyVmT with ErbB3 and p85, as well as the association of ErbB3 with p85 (Figs. 1F–H). Although the molecular determinants of these associations require additional investigation, it is interesting to note that treatment of cells in culture with lapatinib (Fig. 1H) or deletion of ErbB3 in mouse tumors (Fig. 2F) reduced the association of PyVmT with p85, suggesting that PyVmT might be a substrate of ErbB2/ErbB3.

Mutations in PyVmT that abrogate its interaction with Shc (*Y250F* mutation) and p85 (*Y315/322F* mutation) have confirmed that association with these signal transducers is required for oncogene-induced mammary tumor formation (18). However, mice expressing the Y250F and Y315/322F mutants eventually formed focal mammary tumors with markedly delayed latency. Loss of the PI3K binding sites in PyVmT resulted in highly apoptotic and cystic ductal hyperplasias and delayed tumor latency (18), a phenotype strikingly similar to MMTV–PyVmT mammary glands lacking ErbB3 (shown in Fig. 2A and D). Notably, the tumors that occurred in Y250F and Y315/322F expressed markedly elevated levels of ErbB2/ErbB3, suggesting that ErbB2/ErbB3 dimers complement Y250F by engaging Shc and Y315/Y322 by engaging PI3K. Although ErbB2 and ErbB3 can both engage Shc directly upon tyrosine phosphorylation (49), it remains unknown whether ErbB2/ErbB3-induced Shc signaling in the Y250F mutant occurred independently of PyVmT or as part of a complex also containing Shc and PyVmT. Addressing these questions will require additional investigation beyond the scope of the results shown.

In summary, we show in this article that ErbB2/ErbB3 receptors are part of a PyVmT-containing signaling complex that induces PI3K/Akt signaling leading to mammary cell transformation and tumor progression. We also that downregulation of ErbB3 expression using genetic and pharmacologic approaches prevented the formation and decreased growth of established transgenic mammary tumors driven by middle T. Similar results were observed in ErbB2-overexpressing human breast cancer cells in culture. Taken together, these findings support further investigation into different approaches to inhibit ErbB3 function in PI3K-dependent cancers.

Disclosure of Potential Conflicts of Interest

Y. Zhang, Y. Wu, L. Greenberger, and I.D. Horak are employees of Enzon Pharmaceuticals.

Grant Support

This work was supported by NCI R01 grants CA143126 (R.S. Cook) and CA80195 (C.L. Arteaga), Susan G. Komen for the Cure Grant KG100677 (R.S. Cook), ACS Clinical Research Professorship Grant CRP-07-234 (C.L. Arteaga), the Lee Jeans Translational Breast Cancer Research Program (C.L. Arteaga), Breast Cancer Specialized Program of Research Excellence (SPORE) P50 CA98131, and Vanderbilt–Ingram Cancer Center Support Grant P30 CA68485. J.T. Garrett is partially supported by grant T32DK007563 as well as ACS 118813-PF-10-070-01-TBG and DOD BC093376 postdoctoral fellowship awards. A. Chakrabarty is partially supported by postdoctoral fellowship award KG091215 from the Susan G. Komen Breast Cancer Foundation.

The costs of publication of this article were defrayed in part by the payment of page charges. This article must therefore be hereby marked *advertisement* in accordance with 18 U.S.C. Section 1734 solely to indicate this fact.

Received October 20, 2010; revised February 17, 2011; accepted March 22, 2011; published OnlineFirst April 11, 2011.

References

1. Engelman JA, Luo J, Cantley LC. The evolution of phosphatidylinositol 3-kinases as regulators of growth and metabolism. Nat Rev Genet 2006;7:606–19.
2. Bachman KE, Argani P, Samuels Y, Silliman N, Ptak J, Szabo S, et al. The PIK3CA gene is mutated with high frequency in human breast cancers. Cancer Biol Ther 2004;3:772–5.
3. Buttitta F, Felicioni L, Barassi F, Martella C, Paolizzi D, Fresu G, et al. PIK3CA mutation and histological type in breast carcinoma: high frequency of mutations in lobular carcinoma. J Pathol 2006;208:350–5.
4. Campbell IG, Russell SE, Choong DY, Montgomery KG, Ciavarella ML, Hooi CS, et al. Mutation of the PIK3CA gene in ovarian and breast cancer. Cancer Res 2004;64:7678–81.
5. Levine DA, Bogomolniy F, Yee CJ, Lash A, Barakat RR, Borgen PI, et al. Frequent mutation of the PIK3CA gene in ovarian and breast cancers. Clin Cancer Res 2005;11:2875–8.
6. Samuels Y, Wang Z, Bardelli A, Silliman N, Ptak J, Szabo S, et al. High frequency of mutations of the PIK3CA gene in human cancers. Science 2004;304:554.
7. Li J, Yen C, Liaw D, Podsypanina K, Bose S, Wang SI, et al. PTEN, a putative protein tyrosine phosphatase gene mutated in human brain, breast, and prostate cancer. Science 1997;275:1943–7.
8. Stern DF. ERBB3/HER3 and ERBB2/HER2 duet in mammary development and breast cancer. J Mammary Gland Biol Neoplasia 2008;13:215–23.
9. Brugge J, Hung MC, Mills GB. A new mutational AKTivation in the PI3K pathway. Cancer Cell 2007;12:104–7.
10. Manning BD, Cantley LC. AKT/PKB signaling: navigating downstream. Cell 2007;129:1261–74.
11. Guy CT, Cardiff RD, Muller WJ. Induction of mammary tumors by expression of polyomavirus middle T oncogene: a transgenic mouse model for metastatic disease. Mol Cell Biol 1992;12:954–61.
12. Bolen JB, Amini S, DeSeau V, Reddy S, Shalloway D. Analysis of polyomavirus middle-T-antigen-transformed rat cell variants expressing different levels of pp60c-src. J Virol 1987;61:1079–85.
13. Ursini-Siegel J, Schade B, Cardiff RD, Muller WJ. Insights from transgenic mouse models of ERBB2-induced breast cancer. Nat Rev Cancer 2007;7:389–97.
14. Schaffhausen BS, Roberts TM. Lessons from polyoma middle T antigen on signaling and transformation: a DNA tumor virus contribution to the war on cancer. Virology 2009;384:304–16.
15. Dilworth SM. Polyoma virus middle T antigen and its role in identifying cancer-related molecules. Nat Rev Cancer 2002;2:951–6.
16. Ichaso N, Dilworth SM. Cell transformation by the middle T-antigen of polyoma virus. Oncogene 2001;20:7908–16.
17. Rauh MJ, Blackmore V, Andrechek ER, Tortorice CG, Daly R, Lai VK, et al. Accelerated mammary tumor development in mutant polyomavirus middle T transgenic mice expressing elevated levels of either the Shc or Grb2 adapter protein. Mol Cell Biol 1999;19:8169–79.
18. Webster MA, Hutchinson JN, Rauh MJ, Muthuswamy SK, Anton M, Tortorice CG, et al. Requirement for both Shc and phosphatidylinositol 3′ kinase signaling pathways in polyomavirus middle T-mediated mammary tumorigenesis. Mol Cell Biol 1998;18:2344–59.
19. Brantley-Sieders DM, Zhuang G, Hicks D, Fang WB, Hwang Y, Cates JM, et al. The receptor tyrosine kinase EphA2 promotes mammary adenocarcinoma tumorigenesis and metastatic progression in mice by amplifying ErbB2 signaling. J Clin Invest 2008;118:64–78.

Published OnlineFirst April 11, 2011; DOI: 10.1158/0008-5472.CAN-10-3775

20. Lin EY, Jones JG, Li P, Zhu L, Whitney KD, Muller WJ, et al. Progression to malignancy in the polyoma middle T oncoprotein mouse breast cancer model provides a reliable model for human diseases. Am J Pathol 2003;163:2113–26.
21. Kraus MH, Issing W, Miki T, Popescu NC, Aaronson SA. Isolation and characterization of ERBB3, a third member of the ERBB/epidermal growth factor receptor family: evidence for overexpression in a subset of human mammary tumors. Proc Natl Acad Sci U S A 1989;86: 9193–7.
22. Holbro T, Beerli RR, Maurer F, Koziczak M, Barbas CF 3rd, Hynes NE. The ErbB2/ErbB3 heterodimer functions as an oncogenic unit: ErbB2 requires ErbB3 to drive breast tumor cell proliferation. Proc Natl Acad Sci U S A 2003;100:8933–8.
23. Alimandi M, Romano A, Curia MC, Muraro R, Fedi P, Aaronson SA, et al. Cooperative signaling of ErbB3 and ErbB2 in neoplastic transformation and human mammary carcinomas. Oncogene 1995;10:1813–21.
24. Hellyer NJ, Cheng K, Koland JG. ErbB3 (HER3) interaction with the p85 regulatory subunit of phosphoinositide 3-kinase. Biochem J 1998;333:757–63.
25. Carraway KL 3rd, Soltoff SP, Diamonti AJ, Cantley LC. Heregulin stimulates mitogenesis and phosphatidylinositol 3-kinase in mouse fibroblasts transfected with ErbB2/Neu and ErbB3. J Biol Chem 1995;270:7111–6.
26. Muller WJ, Sinn E, Pattengale PK, Wallace R, Leder P. Single-step induction of mammary adenocarcinoma in transgenic mice bearing the activated *c-neu* oncogene. Cell 1988;54:105–15.
27. Muraoka RS, Dumont N, Ritter CA, Dugger TC, Brantley DM, Chen J, et al. Blockade of TGF-beta inhibits mammary tumor cell viability, migration, and metastases. J Clin Invest 2002;109:1551–9.
28. Muraoka RS, Lenferink AE, Law B, Hamilton E, Brantley DM, Roebuck LR, et al. ErbB2/Neu-induced, cyclin D1-dependent transformation is accelerated in p27-haploinsufficient mammary epithelial cells but impaired in p27-null cells. Mol Cell Biol 2002;22:2204–19.
29. Qu S, Rinehart C, Wu HH, Wang SE, Carter B, Xin H, et al. Gene targeting of ErbB3 using a Cre-mediated unidirectional DNA inversion strategy. Genesis 2006;44:477–86.
30. Wagner KU, Wall RJ, St-Onge L, Gruss P, Wynshaw-Boris A, Garrett L, et al. Cre-mediated gene deletion in the mammary gland. Nucl Acids Res 1997;25:4323–30.
31. Guo ZM, Xu K, Yue Y, Huang B, Deng XY, Zhong NQ, et al. Temporal control of Cre recombinase-mediated *in vitro* DNA recombination by *Tet-on* gene expression system. Acta Biochim Biophys Sin (Shanghai) 2005;37:133–8.
32. Gunther EJ, Belka GK, Wertheim GB, Wang J, Hartman JL, Boxer RB, et al. A novel doxycycline-inducible system for the transgenic analysis of mammary gland biology. FASEB J 2002;16:283–92.
33. Guy CT, Webster MA, Schaller M, Parsons TJ, Cardiff RD, Muller WJ. Expression of the neu protooncogene in the mammary epithelium of transgenic mice induces metastatic disease. Proc Natl Acad Sci U S A 1992;89:10578–82.
34. Xia W, Mullin RJ, Keith BR, Liu LH, Ma H, Rusnak DW, et al. Anti-tumor activity of GW572016: a dual tyrosine kinase inhibitor blocks EGF activation of EGFR/erbB2 and downstream Erk1/2 and AKT pathways. Oncogene 2002;21:6255–63.
35. Liao B, Zhang Y, Kosek J, et al. EZN-3920, an LNA antisense oligonucleotide RNA antagonist, down modulates HER3 expression and PI3K/Akt signaling pathway and enhances antiproliferative effect of gefitinib in tumor cells. In: Poster presentation at the 100th American Association for Cancer Research (AACR) Meeting; 2009 Apr 21; Denver, CO. Abstract 4630.
36. Arora A, Kaur H, Wengel J, Maiti S. Effect of locked nucleic acid (LNA) modification on hybridization kinetics of DNA duplex. Nucleic Acids Symp Ser (Oxf) 2008;52:417–8.
37. Kauppinen S, Vester B, Wengel J. Locked nucleic acid: high-affinity targeting of complementary RNA for RNomics. Handb Exp Pharmacol 2006;173:405–22.
38. Veedu RN, Wengel J. Locked nucleic acid as a novel class of therapeutic agents. RNA Biol 2009;6:321–3.
39. Wahlestedt C, Salmi P, Good L, Kela J, Johnsson T, Hokfelt T, et al. Potent and nontoxic antisense oligonucleotides containing locked nucleic acids. Proc Natl Acad Sci U S A 2000;97:5633–8.
40. Baselga J, Swain SM. Novel anticancer targets: revisiting ERBB2 and discovering ERBB3. Nat Rev Cancer 2009;9:463–75.
41. Lee-Hoeflich ST, Crocker L, Yao E, Pham T, Munroe X, Hoeflich KP, et al. A central role for HER3 in HER2-amplified breast cancer: implications for targeted therapy. Cancer Res 2008;68:5878–87.
42. Engelman JA, Zejnullahu K, Mitsudomi T, Song Y, Hyland C, Park JO, et al. MET amplification leads to gefitinib resistance in lung cancer by activating ERBB3 signaling. Science 2007;316:1039–43.
43. Schoeberl B, Faber AC, Li D, Liang MC, Crosby K, Onsum M, et al . An ErbB3 antibody, MM-121, is active in cancers with ligand-dependent activation. Cancer Res 2010;70:2485–94.
44. DeGrendele H. The anti-HER2 monoclonal antibody pertuzumab may be effective in androgen-independent prostate cancer. Clin Prostate Cancer 2003;2:143–5.
45. Sheng Q, Liu X, Fleming E, Yuan K, Piao H, Chen J, et al. An activated ErbB3/NRG1 autocrine loop supports *in vivo* proliferation in ovarian cancer cells. Cancer Cell 2010;17:298–310.
46. Baselga J, Gelmon KA, Verma S, Wardley A, Conte P, Miles D, et al. Phase II trial of pertuzumab and trastuzumab in patients with human epidermal growth factor receptor 2-positive metastatic breast cancer that progressed during prior trastuzumab therapy. J Clin Oncol 2010;28:1138–44.
47. Kristjansdottir K, Dizon D. HER-dimerization inhibitors: evaluating pertuzumab in women's cancers. Expert Opin Biol Ther 2010;10: 243–50.
48. Kunii K, Davis L, Gorenstein J, Hatch H, Yashiro M, Di Bacco A, et al. FGFR2-amplified gastric cancer cell lines require FGFR2 and Erbb3 signaling for growth and survival. Cancer Res 2008;68:2340–8.
49. Yarden Y, Sliwkowski MX. Untangling the ErbB signalling network. Nat Rev Mol Cell Biol 2001;2:127–37.

Cancer Research
The Journal of Cancer Research (1916–1930) | The American Journal of Cancer (1931–1940)

AACR American Association for Cancer Research

ErbB3 Ablation Impairs PI3K/Akt-Dependent Mammary Tumorigenesis

Rebecca S. Cook, Joan T. Garrett, Violeta Sánchez, et al.

Cancer Res 2011;71:3941-3951. Published OnlineFirst April 11, 2011.